

# Comparing LBP, HOG and Deep Features for Classification of Histopathology Images

Taha J. Alhindi<sup>1,2,3</sup>, Shivam Kalra<sup>\*1,3</sup>, Ka Hin Ng<sup>3</sup>, Anika Afrin<sup>4</sup>, Hamid R. Tizhoosh<sup>1</sup>

<sup>1</sup> *Kimia Lab, University of Waterloo, Canada*

<sup>2</sup> *Dept. of Industrial Eng., King Abdulaziz Univ., Jeddah, Saudi Arabia*

<sup>3</sup> *Systems Design Engineering, University of Waterloo, Canada*

<sup>4</sup> *Electrical and Computer Engineering, University of Waterloo, Canada*  
{shivam.kalra, talhindi, kh7ng, aaftrin, tizhoosh}@uwaterloo.ca

**Abstract**—Medical image analysis has become a topic under the spotlight in recent years. There is a significant progress in medical image research concerning the usage of machine learning. However, there are still numerous questions and problems awaiting answers and solutions, respectively. In the present study, comparison of three classification models is conducted using features extracted using local binary patterns, the histogram of gradients, and a pre-trained deep network. Three common image classification methods, including support vector machines, decision trees, and artificial neural networks are used to classify feature vectors obtained by different feature extractors. We use KIMIA Path960, a publicly available dataset of 960 histopathology images extracted from 20 different tissue scans to test the accuracy of classification and feature extractions models used in the study, specifically for the histopathology images. SVM achieves the highest accuracy of 90.52% using local binary patterns as features which surpasses the accuracy obtained by deep features, namely 81.14%.

## I. INTRODUCTION

IN recent years, machine learning has become a popular topic and its applications are increasing day by day with respect to image-based diagnosis, disease prediction and risk assessment [1]. Machine learning is considered a sub-area of artificial intelligence, a set of methods which learn from past data to generalize to new data, can handle noisy input and complex data environments, use prior knowledge, and can form new concepts [2].

After recent success of machine learning, and specially deep learning, in various application fields, some approaches are providing solutions with good accuracy for medical imaging making it a great opportunity for future applications in the healthcare sector. Major experimentation attempts for computer-aided diagnosis had begun in the mid-1980s when the primary focus was on the techniques for detecting lesions on chest radiographs and mammograms [3]. In recent years, machine-learning approaches are being used successfully in the area of image-based disease detection and forecasting. Oliver et al. proposed an approach for reducing false positives for recognition of mammography images using local binary pattern (LBP) in 2007 [4]. LBP was used for

extracting the descriptors and detected masses were classified into either malignant or benign with support vector machines (SVM). The result of the experiment showed that the LBP features were successful in not only in terms of false positive reduction but also it was efficient compared to other methods for diverse mass areas, which is an acute feature of the systems for mass detection. An appraisal of bag-of-features approach for classifying histopathology images had been proposed by Caicedo et al. in 2009 [5]. The key advantage of their proposed framework is that it is focusing to the contents of the image group particularly. This property is achieved by an automated codebook construction and the visual feature descriptors.

An image analysis methodology using SVM classifier to differentiate low and high grades of breast cancer automatically has been proposed by Doyle et al. in 2008 [6]. The dataset contained 48 breast biopsy tissue images having over 3400 image features. After the feature dimensionality reduction and SVM classification, the system achieved an accuracy of 95.8% in differentiating cancerous from non-cancerous cases where Gabor filter features had been used. Distinguishing high-level from low-level cancer was done with architectural features and an accuracy of 93.3% was achieved. Moreover, they used spectral clustering to visualize the hidden manifold form which consists various grades of cancer, and it showed a steady shift from low-grade to high-grade breast cancer.

Kumar et al. conducted a recent study which compares deep features, bag-of-visual-words (BoVW) and LBP for the classification of histopathology image dataset, KIMIA Path960. The classification accuracy obtained in the study using LBP and deep features were 90.62% and 94.72%, respectively, whereas BoVW achieved the highest accuracy of 96.50% [7].

In the present study, comparison of three classification models is conducted. The dataset used is KIMIA Path960 [7]. The models use one of the following feature extractors: Local binary pattern (LBP), histogram of gradients (HOG) and deep features from VGG 19, a pre-trained deep network. The feature vectors are then provided as an input to train

\*Shivam Kalra is a corresponding author for the research work.

several classifiers, for this paper, SVM, decision trees (DTs), and Artificial Neural Networks (ANNs, which use a shallow multi-layer-perceptron) have been selected. The study will empirically justify applications of various feature extraction models and classification methods that are commonly available for the histopathology image analysis.

The study is divided into 5 sections, where feature extractors and classification algorithms are discussed in Section II. The dataset is introduced in Section III. Section IV explains the methodology used in the study. Experiments and results are discussed in Section IV later. Conclusions are drawn in Section V.

## II. BACKGROUND

### A. Feature Extractors

**Local Binary Pattern (LBP):** LBP was introduced in 1994 [8]. Yet, the texture spectrum model of LBP was proposed even earlier in 1990 [9]. LBP feature extractor has been applied in many areas after Ojala and Pietikainen's research in multi-resolution approach in 2002 [10], including text identification [11] and face recognition [5]. Wang has combined LBP with Histogram of Oriented Gradients (HOG) descriptor to improve detection performance in [12].

Classical LBP feature extractor should follow specific actions; these actions are summarized in Fig. 1 [7].

There are series of attempts to improve the LBP method. One recent version finds the intensity values of points in a circular neighborhood by considering the values which have small circular neighborhoods around the central pixel [13].

**Histogram of Oriented Gradients (HOG):** HOG captures features by counting the occurrence of gradient orientation. Traditional HOG divides the image into different cells and computes a histogram of gradient orientations over them [13]. HOG is being applied extensively in object recognition areas as facial recognition[14]. The process for computing HOG is explained in Fig. 2 [15].

**VGG:A Pre-Trained Deep Net:** VGG 16 and 19 are deep convolutional networks (ConvNet) architecture first proposed by K. Simonyan and A. Zisserman from Visual Geometry Group of University of Oxford in 2014 [16]. In the paper, an evaluation of very-deep networks for large-scale image classification was carried out: the generic architecture of the network contained a very small convolution filter with small receptive field of  $3 \times 3$  and the convolutional pace was fixed to 1 pixel, while five max-pooling layers carried out the spatial pooling, over a  $2 \times 2$  pixel window, with a convolution step of 2 [16]. There were three fully-connected layers of same configuration: the first and second layers had 4096 channels each, whereas, the third layer contained 1000 channels and performed ILSVRC-2012 dataset classification [16]. The ConvNet configurations analyzed in this study followed the same architecture which only differ in depth: from network A to E where the depths differ from weight layer 11 to 19 [16]. The results of classification experiments in single-scale, multi-scale and multi-crop evaluation shown that a major improvement could be achieved in this proposed

network if the depth was pushed to 16 and to 19 weight layers, which were VGG16 and VGG19 [16].

In recent years, deep learning has been widely used in medical sector in terms of automated cancer and lesion detection. In 2015, Ertosun and Rubin developed a search system basing on deep learning to automatically search and localize masses, where the system contained a classification and a localization engine as well [17]. There are also works applying deep convolution neural network classifiers to mammograms such as AlexNet [18], VGG net [16] and GoogLeNet [19].

Another study on finding breast cancer from lymph node biopsy images has been carried out by Wang, Dayong, et al. [20] in 2016 using deep learning classification models, including GoogLeNet, VGG-16, AlexNet and FaceNet. Combining estimation from deep learning systems with the diagnosis of the human pathologist, the pathologist's area under the receiver operating curve (AUC) was increased to 0.995, representing nearly 85% reduction in human error rate [20], which means that integration of deep learning approaches with the workflow of pathologists could increase the accuracy in cancer diagnosis.

**Radon Features:** Although we do not experiment with them in this study, we have to mention several approaches that have been proposed to use Radon transform for feature extraction [21], [22]. These methods use projections in local neighbourhood to assemble a feature vector or a histogram. The most recent work reports retrieval accuracies using encoded local projections, short ELP histogram, that surpass deep features for histopathology images [22].

### B. Classifiers

**Support Vector Machines (SVM):** SVM is a classifier designed for binary problems with extension to multi-class problems [23]. Cortes and Vapnik firstly introduced SVM in 1995, with the main idea to ensure the network's high generalization ability by mapping inputs non-linearly to high-dimensional feature spaces, where linear decision surfaces were constructed with special properties [24]. The original idea of support vector network was implied for the situation that training data was separable by a hyperplane without error. Later, Cortes and Vapnik introduced the notion of soft-margins such that a minimal subset of error in the training data is permit table, allowing the remaining part of the training data to be separated by constructing an optimal separating hyperplane [24]. Some advantages of the SVM are the generalization of binary and regression forms and notation simplification [23]. SVM uses several kernels such as the polynomial kernel, linear kernel, and the gaussian radial basis function (RBF) kernel [25], [26].

**Decision Trees:** Decision Trees (DTs) are classifiers represented by a flowchart-like tree structure introduced by J. R. Quinlan in 1986 [27]. DTs do neither make any statistical assumption concerning the inputs nor involve scaling of the data, dissimilar to SVM and neural networks. DT models are constructed in terms of a tree structure in which the dataset is broken down into smaller subsets at each branch.

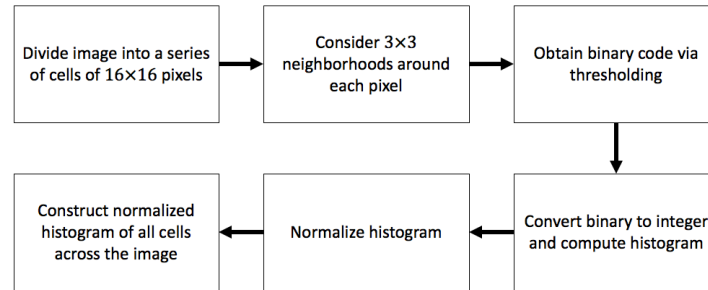


Fig. 1: Flowchart summarizing the main steps of LBP feature extractor.

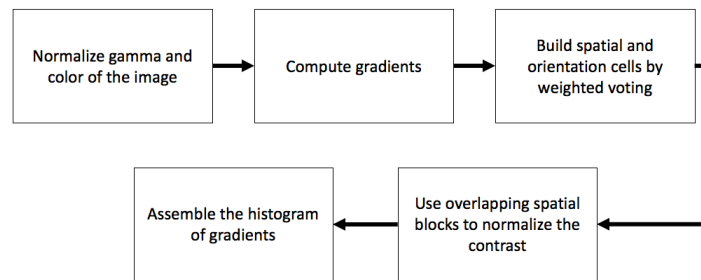


Fig. 2: Flowchart summarizing the process of computing HOG.

Ultimately, the model results in a tree with decision nodes (branches) and leaf nodes. DTs have been used for classification in a variety of domains for pattern recognition with its human-reasoning nature [28]. Breiman has introduced the Classification and Regression Tree (CART) algorithm, which allows continuous values to the model that can be used for regression models [29]. The advantages of the decision trees are self-explanatory logic flow, richness in representing discrete-value classifier, and ability for handling data sets with error and missing data, while the disadvantages are a shortage in classifier interaction and over-sensitivity to irrelevant data and noise [30].

**Artificial Neural Networks (ANNs):** ANNs are neural-network classifiers which simulate the function of the human brain. They are a commonly used machine learning method. The network mainly consists of three primary layers: the first layer represents input neurons; the last layer represents output neurons; a series of weighted middle layers which can minimize the error between actual output and forecasted output [31]. It is difficult to extract rules that ANNs set to interpret the model in the network since it is not to analyze weights and bias terms in the network connections.

When we talk about ANNs we generally mean *shallow networks* (less than 5 layers), in contrast to convolutional neural networks like VGG-19 that are *deep networks*.

### III. IMAGE DATASET

Histopathology images are used as the dataset in this study obtained from the KIMIA Lab<sup>1</sup>, which contains 960

histopathology images that are collected from 400 whole slide images (WSIs) of connective tissue, epithelial, and muscle in a colored TIF format [7]. The dataset has 960 images, which are obtained from 20 selected scans that visually represent different texture/pattern types which are purely based on visual clues. These scans are of the same size from 48 selected regions of interest from WSIs. The images are down-sampled to  $308 \times 168$ . Fig. 3 shows 20 sample images, an image from each class, of the dataset, to illustrate the complexity of the dataset as some of the classes have similar textures while others don't.

#### A. Methodology

For classifying the dataset, three models are constructed based on the features extractor algorithms that are used. The models use LBP and HOG features extractors, respectively.

The feature vectors obtained by each LBP, HOG or VGG19 features extracting models are considered as inputs for the classifying methods, the feature vectors are given independently to SVM, DTs, and ANNs. The accuracies are obtained through the  $k$ -fold cross-validation method where  $k = 3$ .

Python programming language environment is used for conducting the experiments with its supporting libraries provided by Anaconda distributions. Mahotas library [32] is used for LBP features extractor. Scikit-Image [33] library is used for HOG feature extraction and SVM, DT, and ANN classification algorithms.

<sup>1</sup>Source of dataset: <http://kimia.uwaterloo.ca/>

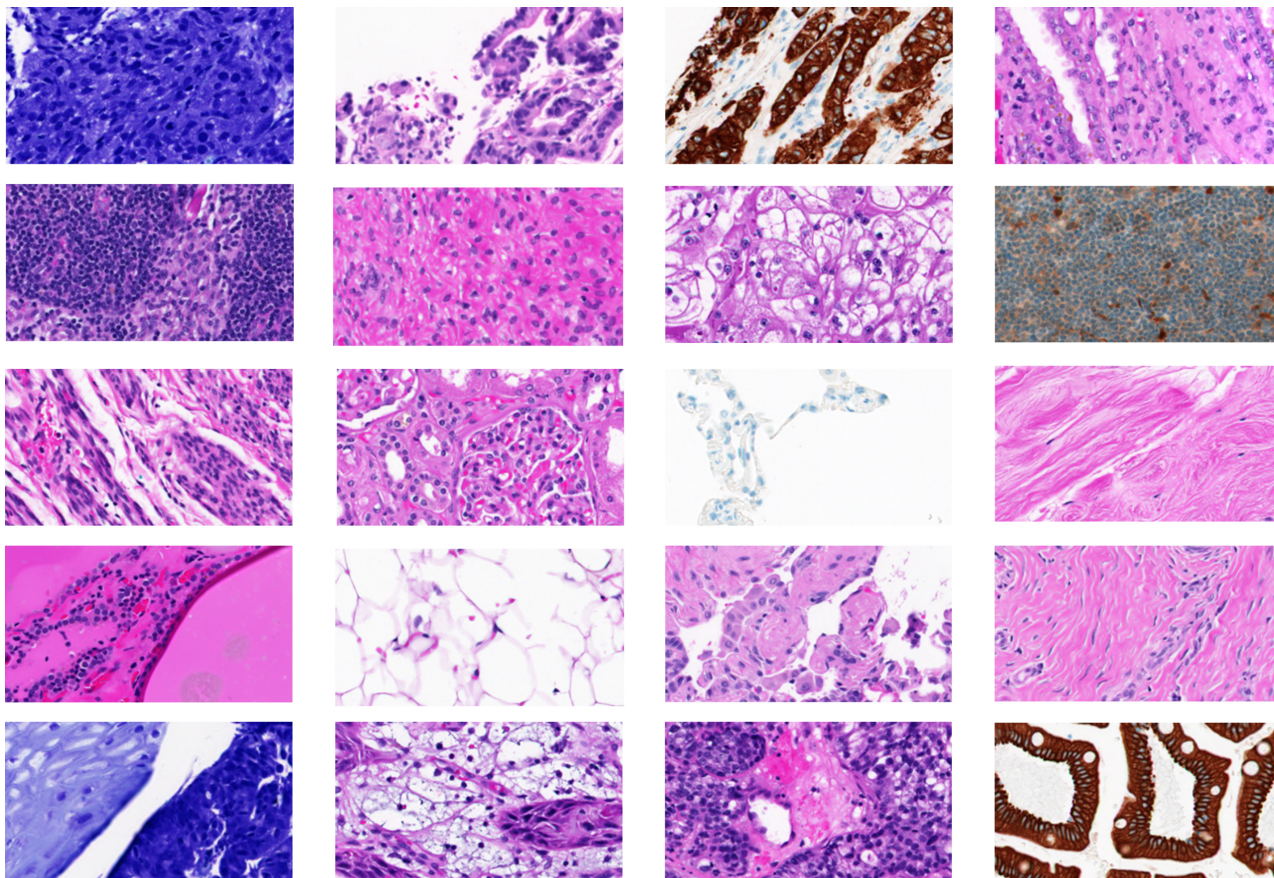


Fig. 3: 20 sample images, one from each class, showing the 20 classes of KIMIA Path 960 image dataset

### B. Feature Extraction with HOG

Image features extraction using HOG is applied in the first model.  $18 \times 18$  cell size and  $1 \times 1$  block size are used for computing the features. The output of the HOG feature extraction is a histogram with 1224 dimensions (bins) for each image. The histograms can be used directly for training the classifiers. A 3-fold cross-validation is performed to obtain the average for SVM, DT, and ANN classification algorithms.

### C. Feature Extraction with LBP

The second feature extraction model uses the LBP algorithm. The feature vectors obtained through the application of LBP are captured in a histograms. The radius parameter used is set to 4 (pixels) and the number of points to consider are set to 14. The resulting histograms will be of 1182 dimensions (bins) for each image. Therefore, these feature vectors can be used directly for training the classifiers. A 3-fold cross-validation method have been used (with same random initialization) in this model to obtain the accuracies for SVM, DT, and ANN.

### D. Deep Feature Extraction with VGG19

Third feature extraction model uses the VGG19 deep network. Features for the given pathology images are extracted

from four different layers within VGG19 network which contains 19 layers in total divided in group of 5 blocks. These four layers are: *fc1*, *block5\_pool*, *block4\_pool*, *block3\_pool*. The reason for choosing multiple locations is because the VGG19 network used for our experiments is pre-trained on natural images using the ImageNet dataset [18]. The natural images provide very different variability compared to the pathology images. However, due to layered construction of VGG19, each layer is responsible for extracting different type of features from an image, hence the deeper we go into the network, the extracted features become more suitable for natural images and lose their generality for other type of images such as histopathology images. We also find this behaviour to be true, which will be discussed in Section IV.

We extracted 4 feature sets from the VGG-19 for Kimia Path960 dataset, and without losing generality, we performed same steps as before in order to calculate accuracies for each of the classification models. One may argue that, using ANNs on features extracted using VGG19 could be considered as fine-tuning, however, for all our experiments, we are treating classification methods separate from feature extraction models. Once each of our feature extraction model provides its corresponding features, we apply same classification methods on these features to calculate their discriminating power.

## IV. EXPERIMENTS AND RESULTS

## A. LBP Results

The model that uses LBP features obtained the highest results in our experiments. The accuracy is reported at 90.52% using SVM which has a gamma value of 0.0000015 and penalty parameter of the error term  $C = 2.5$  while using the RBF kernel. The ANN classifier for LBP features consists of 300 neurons at the first and second layers and has a learning rate of 0.0005. In contrast, the DT classifier achieved an accuracy of 66.35%. The second row in Table I summarizes the accuracies obtained by the LBP features extractor classification model using SVM, DT, and ANN methods (highest accuracy is highlighted in bold).

Fig. 4 and Fig. 5 plot the learning curves of the SVM and ANN models that use LBP features. The lines in the figures are the mean values of the scores and the highlighted area around the lines is the range of its standard deviation, respectively. The red color is used for training scores while the green color is used for the testing scores.

Fig. 4 shows that the training score was consistently high through the iterations. However, the testing scores were improving while the training iterations were increasing. Fig. 5 illustrates that the training score of the ANN classifier has reached its high-point at around training iteration 500. However, the testing score kept increasing till it reaches roughly 660 iterations.

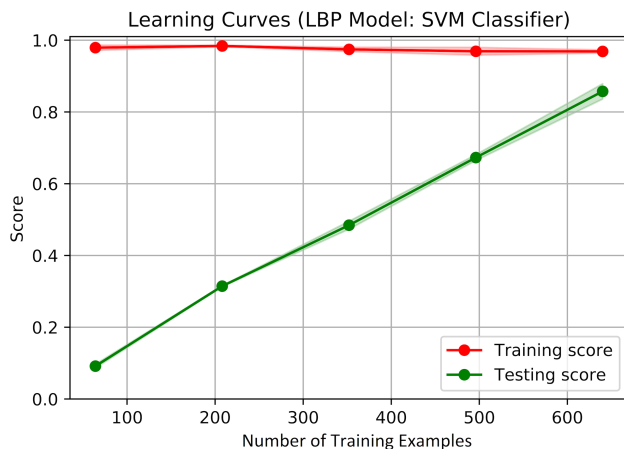


Fig. 4: Plot of the SVM learning curves using LBP features.

## B. HOG Results

The histograms obtained by HOG feature extraction consisted of 1224 bins for each image. The accuracies achieved by HOG features model are the lowest compared to the other models. The SVM method resulted in 4.79% accuracy. The DT classifier computed 13.13% accuracy and the ANN classifier achieved 36.15%. All these classifiers had the same parameters as the classifier of the LBP features classification model. Table I summarizes the accuracies obtained by the SVM, DT, and ANN classifiers with HOG features.

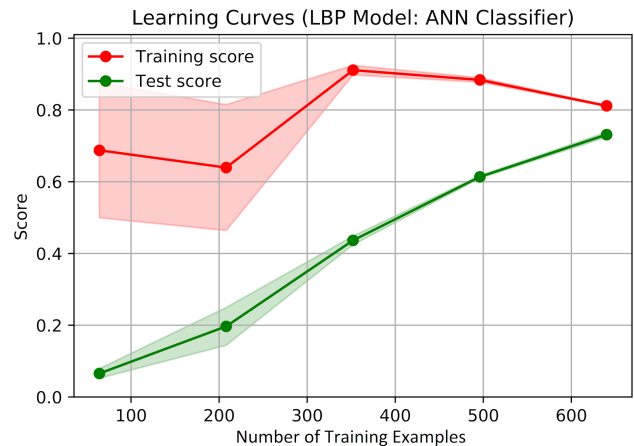


Fig. 5: Plot of the ANN learning curves using LBP features.

## C. Deep Features Results

Feature vectors extracted from the later layers of VGG 19, for example *fc1* and *block5\_pool*, do not perform well for the pathology images. The highest accuracy on features obtained from these two layers is achieved using DT classifier, 44.79 and 47.18, respectively. The reason DT classifier dominates SVM or ANN is because of the high sparsity of the feature vectors. Features from the *block4\_pool* contribute to the highest accuracy among deep features and are the second highest overall. However, comparing the feature's dimensionality, its almost half the dimension of the feature from LBP.

## V. CONCLUSION

The experiments conducted on KIMIA Path960 dataset using LBP, HOG and deep network's features show that LBP feature extractor has outperformed the other methods, especially while using SVM algorithm as a classifier. However, the results obtained by HOG feature extractor were not satisfactory as the model has under-performed by the parameters used in the present study. However, these parameter choices were made to stay consistent in terms of feature's dimensions across the multiple feature extractor models.

Table II summarizes feature dimensions, classifier yielding best accuracies and value of the best accuracies obtained by all three of the feature extraction models.

The DTs have underperformed compared to SVM and ANN classifiers in most of the cases except when features were sparse, for example in case VGG 19 (*block5\_pool*) and VGG 19 (*fc1*) as in Table II. Meanwhile, SVM algorithm has shown good results for overall except for highly sparse features. Therefore, one conclusion to be made is that selection between DT and SVM must be made depending on the sparsity of feature vectors. The ANN algorithm had the best accuracy using HOG features, which is the highest among all three classifiers, otherwise ANN is classifier is generally under performing with high standard deviation.

Feature Extraction Models		Classification Algorithms		
		SVM	DT	ANN
LBP	Fold 1	<b>91.56%</b>	65.31%	77.50%
	Fold 2	<b>88.75%</b>	66.25%	76.25%
	Fold 3	<b>91.25%</b>	67.50%	75.10%
	All Folds	<b>90.52 ± 1.26%</b>	66.35 ± 0.90%	75.10 ± 2.56%
HOG	Fold 1	3.44%	11.25%	<b>36.25%</b>
	Fold 2	7.81%	13.44%	<b>35.94%</b>
	Fold 3	3.13%	14.69%	<b>36.25%</b>
	All Folds	4.79 ± 2.14%	13.13 ± 1.42%	<b>36.15 ± 0.15%</b>
VGG19 (fc1)	Fold 1	9.37%	<b>45.31%</b>	5.62%
	Fold 2	9.68%	<b>45.93%</b>	1.25%
	Fold 3	9.06%	<b>43.12%</b>	4.37%
	All Folds	9.37 ± 0.25%	<b>44.79 ± 1.2%</b>	7.50 ± 1.83%
VGG19 (block5_pool)	Fold 1	8.75%	<b>48.75%</b>	16.87%
	Fold 2	5.93%	<b>47.50%</b>	18.12%
	Fold 3	4.37%	<b>45.31%</b>	25.00%
	All Folds	6.35 ± 1.81%	<b>47.18 ± 1.42%</b>	20.00 ± 3.57%
VGG19 (block4_pool)	Fold 1	<b>84.68%</b>	59.37%	10.93%
	Fold 2	<b>80.31%</b>	58.43%	17.50%
	Fold 3	<b>78.43%</b>	59.06%	13.12%
	All Folds	<b>81.14 ± 2.61%</b>	58.95 ± 0.39%	13.85 ± 2.73%
VGG19 (block3_pool)	Fold 1	<b>67.81%</b>	62.81%	2.81%
	Fold 2	<b>67.81%</b>	70.31%	5.62%
	Fold 3	66.87%	<b>72.18%</b>	6.25%
	All Folds	67.49 ± 0.44%	<b>68.43 ± 4.2%</b>	4.90 ± 1.49%

TABLE I: The 3-fold cross-validation accuracies for LBP, HOG, VGG19 features using SVM, DT, and ANN classifiers.

Feature Extraction Models	Feature Size	Best Accuracy Achieved	Best Classification Method
LBP	1182	<b>90.52%</b>	SVM
VGG 19 (block4_pool)	512	81.14%	SVM
VGG 19 (block3_pool)	256	68.43%	DT
VGG 19 (block5_pool)	512	47.18%	DT
VGG 19 (fc1)	4096	44.79%	DT
HOG	1224	34.37%	ANN

TABLE II: Show the best accuracies values, best classification methods and length of feature vectors for each feature extractor model. The best accuracy is achieved by LBP feature extractor using SVM classifier and second best is by VGG 19 (block4\_features) using SVM as well.

The accuracies obtained by HOG features extractor may be improved further by changing the parameters of the algorithm. However, it required a lot of resources to conduct these experiments. Furthermore, fine-tuning VGG 19 by cutting it after block3\_pool may offer more improvements in accuracies on pathology datasets as well.

Of course, that a handcrafted feature vector like LBP, with very simple implementation, can beat deep features is a surprising result considering how much efforts go into designing and training of a deep network. One may say that deep nets need to be trained for the problem at hand with a large number of training images. However, there are many situations where a large, balanced and labelled dataset is not available.

## REFERENCES

- [1] M. de Bruijne, "Machine learning approaches in medical image analysis: From detection to diagnosis," vol. 33, pp. 94–97.
- [2] *AI: Its Nature and Future*. Oxford University Press.
- [3] M. L. Giger, H.-P. Chan, and J. Boone, "Anniversary paper: History and status of CAD and quantitative image analysis: The role of Medical Physics and AAPM," vol. 35, no. 12, pp. 5799–5820.
- [4] A. Oliver, X. Llad, J. Freixenet, and J. Mart, "False Positive Reduction in Mammographic Mass Detection Using Local Binary Patterns," in *Medical Image Computing and Computer-Assisted Intervention MICCAI 2007*, ser. Lecture Notes in Computer Science. Springer, Berlin, Heidelberg, pp. 286–293.
- [5] J. C. Caicedo, A. Cruz, and F. A. Gonzalez, "Histopathology Image Classification Using Bag of Features and Kernel Functions," in *Artificial Intelligence in Medicine*, ser. Lecture Notes in Computer Science. Springer, Berlin, Heidelberg, pp. 126–135.
- [6] S. Doyle, S. Agner, A. Madabhushi, M. Feldman, and J. Tomaszewski,

- “Automated grading of breast cancer histopathology using spectral clustering with textural and architectural image features,” in *2008 5th IEEE International Symposium on Biomedical Imaging: From Nano to Macro*, pp. 496–499.
- [7] M. D. Kumar, M. Babaie, S. Zhu, S. Kalra, and H. R. Tizhoosh, “A Comparative Study of CNN, BoVW and LBP for Classification of Histopathological Images.”
- [8] T. Ojala, M. Pietikainen, and D. Harwood, “Performance evaluation of texture measures with classification based on Kullback discrimination of distributions,” in *Proceedings of 12th International Conference on Pattern Recognition*, vol. 1, pp. 582–585 vol.1.
- [9] D.-c. He and L. Wang, “Texture Unit, Texture Spectrum, And Texture Analysis,” vol. 28, no. 4, pp. 509–512.
- [10] T. Ojala, M. Pietikainen, and T. Maenpaa, “Multiresolution gray-scale and rotation invariant texture classification with local binary patterns,” vol. 24, no. 7, pp. 971–987.
- [11] I. Jung and I. S. Oh, “Local Binary Pattern-Based Features for Text Identification of Web Images,” in *2010 20th International Conference on Pattern Recognition*, pp. 4320–4323.
- [12] X. Wang, T. X. Han, and S. Yan, “An HOG-LBP human detector with partial occlusion handling,” in *2009 IEEE 12th International Conference on Computer Vision*, pp. 32–39.
- [13] “Local Binary Patterns: New Variants and Applications.”
- [14] O. Dniz, G. Bueno, J. Salido, and F. De la Torre, “Face recognition using Histograms of Oriented Gradients,” vol. 32, no. 12, pp. 1598–1603.
- [15] N. Dalal and B. Triggs, “Histograms of oriented gradients for human detection,” in *2005 IEEE Computer Society Conference on Computer Vision and Pattern Recognition (CVPR’05)*, vol. 1, pp. 886–893.
- [16] K. Simonyan and A. Zisserman, “Very Deep Convolutional Networks for Large-Scale Image Recognition.”
- [17] M. G. Ertosun and D. L. Rubin, “Probabilistic visual search for masses within mammography images using deep learning,” in *2015 IEEE International Conference on Bioinformatics and Biomedicine (BIBM)*, pp. 1310–1315.
- [18] A. Krizhevsky, I. Sutskever, and G. E. Hinton, “Imagenet classification with deep convolutional neural networks,” in *Advances in Neural Information Processing Systems*, pp. 1097–1105.
- [19] C. Szegedy, W. Liu, Y. Jia, P. Sermanet, S. Reed, D. Anguelov, D. Erhan, V. Vanhoucke, and A. Rabinovich, “Going Deeper with Convolutions.”
- [20] D. Wang, A. Khosla, R. Gargeya, H. Irshad, and A. H. Beck, “Deep Learning for Identifying Metastatic Breast Cancer.”
- [21] M. Babaie, H. Tizhoosh, A. Khatami, and M. Shiri, “Local radon descriptors for image search,” *arXiv preprint arXiv:1710.04097*, 2017.
- [22] H. Tizhoosh and M. Babaie, “Representing medical images with encoded local projections,” *IEEE Transactions on Biomedical Engineering*, pp. 1–1, 2018.
- [23] R. Begg, D. T. Lai, and M. Palaniswami. *Computational Intelligence in Biomedical Engineering*.
- [24] C. Cortes and V. Vapnik, “Support-vector networks,” vol. 20, no. 3, pp. 273–297.
- [25] B. Scholkopf, K. Tsuda, and J.-P. Vert. *Kernel Methods in Computational Biology*.
- [26] K.-j. Kim, “Financial time series forecasting using support vector machines,” vol. 55, no. 1, pp. 307–319.
- [27] J. R. Quinlan, “Induction of decision trees,” vol. 1, no. 1, pp. 81–106.
- [28] *Automatic Design of Decision-Tree Induction Algorithms — Rodrigo C. Barros — Springer*.
- [29] L. Breiman, J. Friedman, C. J. Stone, and R. Olshen. *Classification and Regression Trees*.
- [30] L. Rokach and O. Maimon, “Top-down induction of decision trees classifiers - a survey,” vol. 35, no. 4, pp. 476–487.
- [31] W.-C. Wang, K.-W. Chau, C.-T. Cheng, and L. Qiu, “A comparison of performance of several artificial intelligence methods for forecasting monthly discharge time series,” vol. 374, no. 3, pp. 294–306.
- [32] L. P. Coelho, “Mahotas: Open source software for scriptable computer vision,” vol. 1, no. 1, p. e3.
- [33] S. van der Walt, J. L. Schnberger, and et. al. *Scikit-image: Image processing in Python [PeerJ]*.